J. Chem. Sci., Vol. 118, No. 6, November 2006, pp. 513–518.

Reverse micellar synthesis and properties of nanocrystalline GMR materials ($LaMnO_3$, $La_{0.67}Sr_{0.33}MnO_3$ and $La_{0.67}Ca_{0.33}MnO_3$): Ramifications of size considerations

TOKEER AHMAD,[1] KANDALAM V RAMANUJACHARY,[2] SAMUEL E LOFLAND[2] and ASHOK K GANGULI[1,*]

[1]Department of Chemistry, Indian Institute of Technology, Hauz Khas, New Delhi 110 016
[2]Centre for Materials Research and Education, Rowan University, 201 Mullica Hill Road, Glassboro, NJ 08028, USA
e-mail: ashok@chemistry.iitd.ernet.in

Abstract. Nanoparticles of complex manganites (viz. $LaMnO_3$, $La_{0.67}Sr_{0.33}MnO_3$ and $La_{0.67}Ca_{0.33}MnO_3$) have been synthesized using the reverse micellar route. These manganites are prepared at 800°C and the monophasic nature of all the oxides has been established by powder X-ray diffraction studies. TEM studies show an average grain size of 68, 80 and 50 nm for $LaMnO_3$, $La_{0.67}Sr_{0.33}MnO_3$ and $La_{0.67}Ca_{0.33}MnO_3$ respectively. Ferromagnetic ordering is observed at around 250 K for $LaMnO_3$, 350 K for $La_{0.67}Sr_{0.33}MnO_3$ and 200 K for $La_{0.67}Ca_{0.33}MnO_3$. These Curie temperatures correspond well with those reported for bulk materials with similar composition.

Keywords. Reverse micellar synthesis; nanomaterials; magnetism; rare-earth manganites.

1. Introduction

Nanomaterials of perovskite-related manganites have attracted attention due to their applications in devices for magnetic information storage and retrieval. Extensive studies have been carried out in the last ten years on rare earth manganites with perovskite structure, driven by the discovery of giant or colossal magnetoresistance (GMR or CMR) in these compounds. The use of magnetic multilayers with giant magnetoresistance as magnetic reading heads has also been reported.[1,2] These compounds exhibit a very large magnetoresistance in a temperature range that ties in closely with the ferromagnetic Curie temperature of the manganites. Furthermore, doped rare-earth manganese oxides are also popular owing to their potential application as electrode materials in solid oxide fuel cells.[3] $La_{1-x}Sr_xMnO_3$ is currently used as an electrode material in solid oxide fuel cells (SOFCs) because of its high electronic/oxide conductivity, good chemical stability and compatibility with other cell components even at high temperatures of 1000°C.[4] Use of nanostructured materials as electrodes for fuel-cell cathodes is expected to promote catalytic reactions on the surface[5] as they provide larger specific surface area.

Stoichiometric $LaMnO_3$ is an antiferromagnetic insulator; however it is always nonstoichiometric when prepared in air.[6] The presence of Mn^{III}–O–Mn^{IV} pairs in the perovskite structure allows double-exchange, leading to ferromagnetism, metal–insulator transitions, and magnetoresistance in nominal $LaMnO_{3+\gamma}$.[7] With cationic substitutions like Ca^{2+} or Sr^{2+} on the lanthanum site, it shows paramagnetic–ferromagnetic transition coupled to high magnetoresistance ratios.[7,8]

Several methods have been explored for the synthesis of nanomaterials. These processes involve a few physical (like vapour deposition and evaporation-condensation) and chemical methods (hydrothermal, solvothermal and sonochemical etc.).[9–11] Among all the chemical processes, the reverse micellar method has been recently demonstrated as a versatile method[12] to produce a variety of nanoparticles. This method is superior to other synthetic methods as it produces homogeneous, uniform and monodisperse nanosized precursors. The reverse micellar method consists of nano-sized aqueous droplets stabilized by surfactant molecules[13] and has been used extensively for the synthesis of oxide nanoparticles.[14–16] We have extensively used reverse micelles for the synthesis of a variety of ternary and quaternary oxides

*For correspondence

in the recent past.[17–19] There are only few reports[20,21] on the preparation of $LaMnO_3$ via the microemulsion method, and only one brief report on the synthesis of lanthanum–strontium manganites using reverse micellar microemulsion.[22] Using the micro-emulsion route,[20,21] $LaMnO_3$ composition forms with a wide range of particle sizes (20–100 nm) and an average size of ~80 nm. To our knowledge, there is no report available in the literature on the synthesis of lanthanum–calcium manganites using reverse micelles.

In this paper, we report the synthesis of $LaMnO_3$ and its Sr- and Ca-doped analogues with the composition $La_{0.67}Sr_{0.33}MnO_3$ and $La_{0.67}Ca_{0.33}MnO_3$ by a modified reverse micellar route using Tergitol as the surfactant. We have extensively characterized the oxides using X-ray diffraction, transmission electron microscopy (TEM) and electron diffraction (ED) studies. We also report here details of the temperature-dependent magnetization of these manganites.

2. Experimental

0·1 M solutions of La^{3+}, Mn^{2+}, Sr^{2+} and Ca^{2+} in double distilled water were prepared from lanthanum nitrate hexahydrate (Spectrochem), manganese acetate tetrahydrate (CDH), strontium acetate (Aldrich) and calcium nitrate tetrahydrate (Merck) respectively. 3.0 ml each of lanthanum nitrate, manganese acetate and sodium hydroxide (BDH, 97%) were taken in three separate beakers for the synthesis of $LaMnO_3$. To each of the above, 60 ml of cyclohexane (Ranbaxy, LR grade), 7·0 ml Tergitol NP-9 (Aldrich) as the surfactant and 5·2 ml of *n*-octanol (Spectrochem, puriss, 99%) as the co-surfactant were added. These three microemulsions were then mixed and stirred overnight at room temperature. A transparent solution was obtained. On evaporating the solvent from the solution at 60 ± 5°C, a brown precipitate was obtained which was washed with acetone, centrifuged and then dried in an oven at 60°C for 1 h. The powder thus obtained was further heated in air at 500°C for 20 h and subsequently at 800°C for 20 h to get the pure $LaMnO_3$ powders. However, for the synthesis of $La_{0.67}A_{0.33}MnO_3$ (where A = Sr^{2+} and Ca^{2+}), four separate microemulsions were prepared for each composition, three of which contained metal ions and the fourth contained NaOH which acted as the precipitating agent. The stoichiometry in different microemulsion systems was maintained according to the molecular formula. The rest of the procedure was similar to that applied for the synthesis of $LaMnO_3$.

Powder X-ray diffraction studies (PXRD) were carried out on a Bruker D8 Advance diffractometer using Ni filtered CuKα radiation. Normal scans were recorded with a step size of 0·02° and step time of 1 s. Raw data was subjected to background corrections and Kα_2 lines were stripped off. Details of line broadening studies are given elsewhere.[18,19] The cell parameters were determined using a least square fitting procedure on all reflections using quartz as the external standard.

TEM and ED studies were carried out using the Tecnai-20 G2 Transmission Electron Microscope with TWIN LENS configuration, fitted with EDAX Genesis2000 and SUTW Detector and Megaview III CCD camera for image acquisition system. TEM specimens were prepared by dispersing the powder in acetone by ultrasonic treatment, dropping onto a porous carbon film supported on a copper grid, and then drying in air. The magnetization was measured at temperatures in the range 5 to 300 K, in applied fields of up to 5 kOe with a quantum design physical properties measurement system.

3. Results and discussion

X-ray diffraction patterns of the powder were taken after heating at 500 and 800°C. Figure 1a shows the powder X-ray diffraction of $LaMnO_3$ at 800°C. All the observed reflections were indexed on the basis of a cubic cell with the refined cell parameter of a = 3·876(3) Å, which is close to the reported cell parameter of $LaMnO_3$ (JCPDS no. 75-0440). Monophasic $La_{0.67}Sr_{0.33}MnO_3$ could be obtained after heating the precursor at 800°C and the X-ray pattern (figure 1b) could be indexed satisfactorily on the basis of a rhombohedral cell with the refined lattice parameters as a = 5·473(1) Å and c = 13·362(5) Å which are close to the reported cell parameters of rhombohedral $La_{0.67}Sr_{0.33}MnO_{2.91}$ (JCPDS no. 50-0308). The loaded composition of $La_{0.67}Ca_{0.33}MnO_3$ after heating at 800°C shows a slight shift of 0·03° in 2θ towards lower Bragg angles compared to pure $LaMnO_3$. Thus the XRD pattern of $La_{0.67}Ca_{0.33}MnO_3$ (figure 1c) loaded composition could be indexed on the basis of an orthorhombic cell with refined lattice parameters of a = 5·669(3) Å, b = 7·666(5) Å and c = 5·53(7) Å which is quite close to the reported parameters of orthorhombic $La_{0.67}Ca_{0.33}MnO_3$.[23] The small orthorhombic distortion for $La_{1-x}Ca_xMnO_3$,

normally observed with the Ca concentration in the range of $0{\cdot}25 \leq x \leq 0{\cdot}5$ may sometimes be difficult to resolve.[24]

The grain size of $LaMnO_3$ and related oxide nanoparticles were determined using X-ray line broadening and transmission electron microscopic studies. X-ray studies show an average grain size of 55 nm while TEM studies show nearly uniform and slightly agglomerated particles of $LaMnO_3$ having grain size of 68 nm (figure 2a) at 800°C. Figure 2b shows the electron diffraction pattern of $LaMnO_3$ where a large number of spots are arranged in a circular manner, indicating the nanocrystalline nature of lanthanum manganite powder. The average grain size of $La_{0.67}Sr_{0.33}MnO_3$ was found to be around 80 nm (figure 3a) using TEM studies. X-ray studies show average grain size of 62 nm. The grains are larger in size as compared to those of pure $LaMnO_3$, and agglomeration in grains is clearly visible. Dark field image of $La_{0.67}Sr_{0.33}MnO_3$ was also recorded and is shown in the inset of figure 3a. The particles are spherical and distributed uniformly. Electron diffraction micrograph of $La_{0.67}Sr_{0.33}MnO_3$ at 800°C (figure 3b) confirms the nanocrystalline nature.

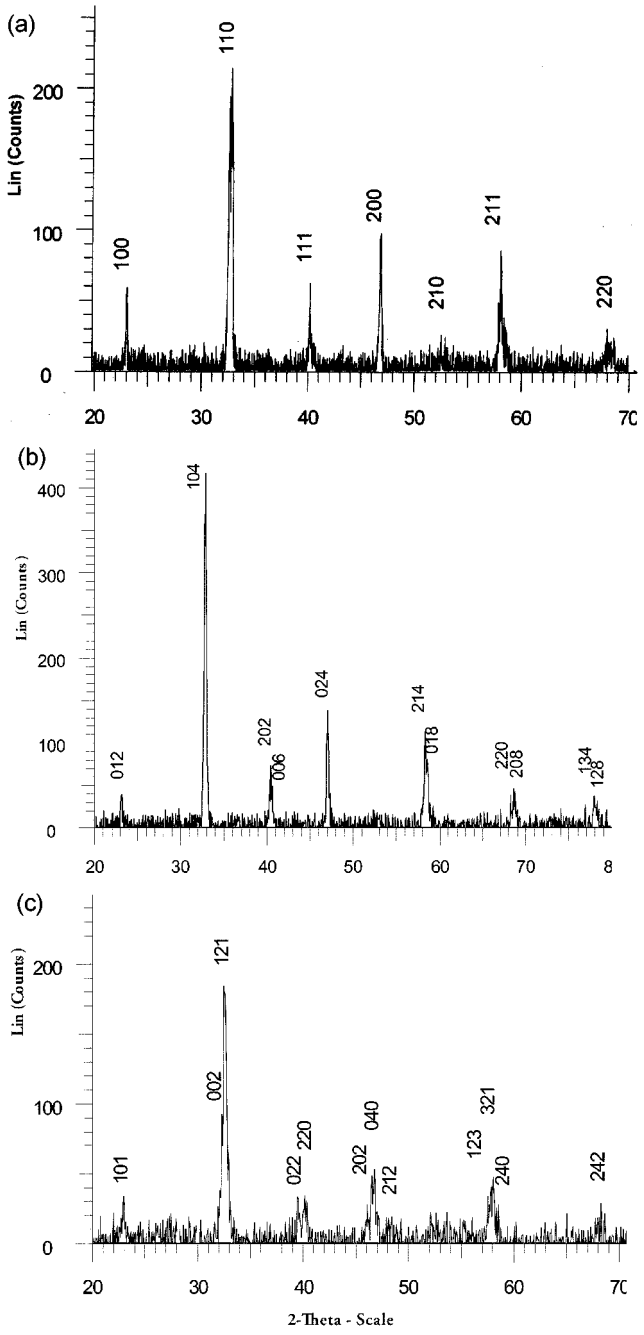

Figure 1. Powder X-ray diffraction pattern of (**a**) $LaMnO_3$, (**b**) $La_{0{\cdot}67}Sr_{0{\cdot}33}MnO_3$ and (**c**) $La_{0{\cdot}67}Ca_{0{\cdot}33}MnO_3$ after calcining at 800°C.

TEM and X-ray line broadening studies have also been carried out on the powders of $La_{0{\cdot}67}Ca_{0{\cdot}33}MnO_3$ obtained at 800°C. The grain size was found to be ~ 50 nm (figure 4a) which is smaller compared to those of $LaMnO_3$ and $La_{0{\cdot}67}Sr_{0{\cdot}33}MnO_3$. The average grain size was found to be 46 nm using Scherrer's formula which is in accordance with the TEM studies. Dark field image of $La_{0{\cdot}67}Ca_{0{\cdot}33}MnO_3$ was also taken and is shown in the inset of figure 4a. The particles are nearly spherical and distributed uniformly. Electron diffraction pattern of $La_{0{\cdot}67}Ca_{0{\cdot}33}MnO_3$ is presented in figure 4b, which shows the nanocrystalline nature of $La_{0{\cdot}67}Ca_{0{\cdot}33}MnO_3$.

The variation of magnetization with temperature (figure 5a) for $LaMnO_3$ is in accordance with literature reports with a ferromagnetic onset temperature around ~ 250K.[7] The small dip in the plot around ~ 45 K can be attributed to the presence of small amounts (~ 1%) of hausmanite (Mn_3O_4). The measured moment of ~ 2·4 BM is smaller than is expected based on the $3d^4$ configuration of Mn^{3+}. This may be related to the paramagnetic nature of the spins residing on the surface/grain boundaries of the nanoparticulate manganates.

Both the Sr- and Ca-doped samples showed ordering temperatures (~ 350 K for Sr and ~ 200 K for Ca) (figures 5b and c), which are consistent with literature reports on similar compositions.[25,26] Note that the onset temperature of 350 K has been obtained by extrapolating the data, since the data were collected up to 300 K. $LaMnO_3$ with a small proportion of Mn^{4+} becomes antiferromagnetically ordered at low temperatures, but when the La site is progressively substituted by a divalent cation like Ca or Sr, the proportion of Mn^{4+} increases and the material be-

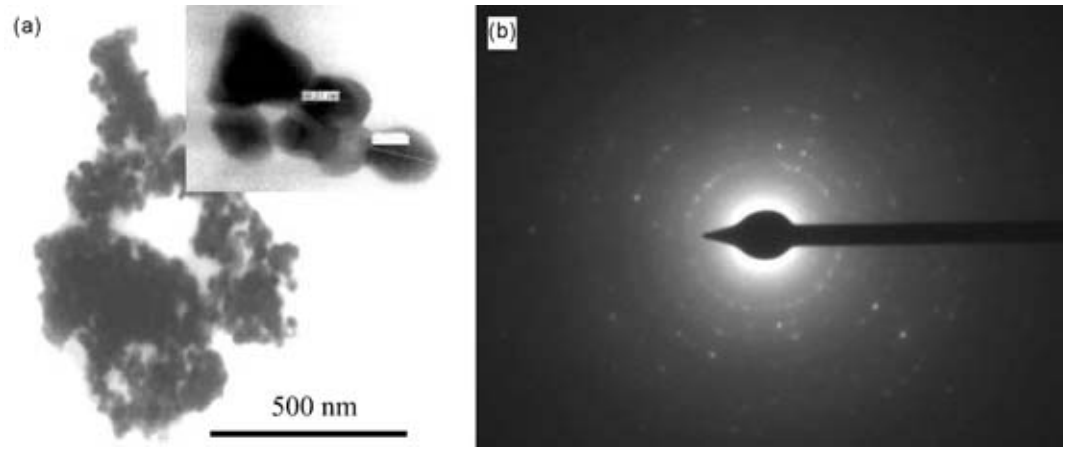

Figure 2. (**a**) TEM and (**b**) electron diffraction micrograph of $LaMnO_3$ powder heated at 800°C. Inset in (a) shows a closer view of the nanoparticles.

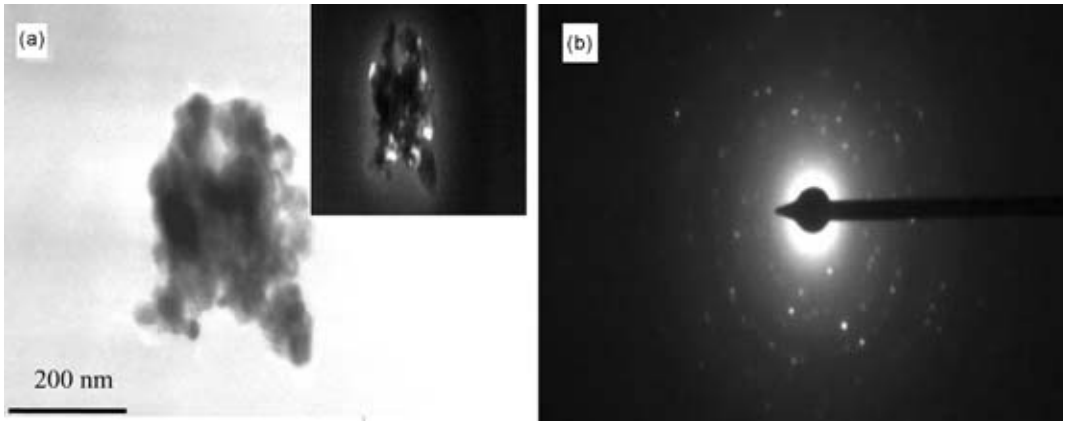

Figure 3. (**a**) TEM and (**b**) electron diffraction micrograph of $La_{0·67}Sr_{0·33}MnO_3$ powder heated at 800°C. Inset in (a) shows the dark field image of nanoparticles.

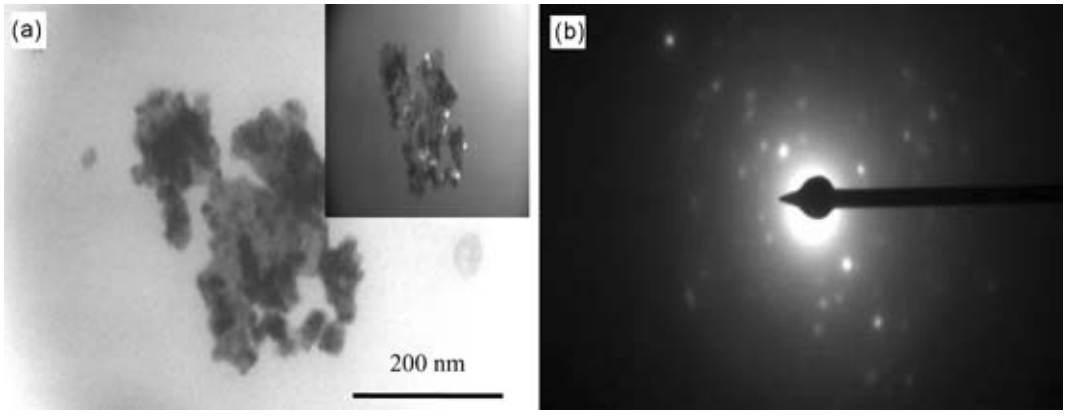

Figure 4. (**a**) TEM and (**b**) electron diffraction micrograph of $La_{0·67}Ca_{0·33}MnO_3$ powder heated at 800°C. Inset in (a) shows the corresponding dark field image.

comes ferromagnetic with a well-defined Curie temperature at a finite value of the concentration of the divalent ion.[27] The effective magnetic moments calculated for all the compositions are in the range of 1·9–2·5 BM, which are considerably smaller than the theoretically predicted moments. Again, the re-

duced moment in the ordered state can be ascribed either to the smaller particle size of the particles with uncompensated spins near the boundaries or large domains of anti-ferromagnetic clusters.

Although not present in the Ca phase, the Sr phase shows a small dip around 45 K, probably due to the presence of the hausmanite phase. This can be ascribed to the higher electropositivity of Sr ions (relative to Ca), which facilitates the formation of Mn_3O_4. Unlike the pure $LaMnO_3$ phase where a well-defined ordering temperature is seen, the Ca- and Sr-substituted phases show a broad transition to the ferromagnetic phase. We attribute this either to an inhomogeneous distribution of M^{2+} ions in the lattice or directly to the smaller size of the particles. Perhaps several high temperature treatments followed by slow annealing might remove this broad feature and give rise to a sharp onset.

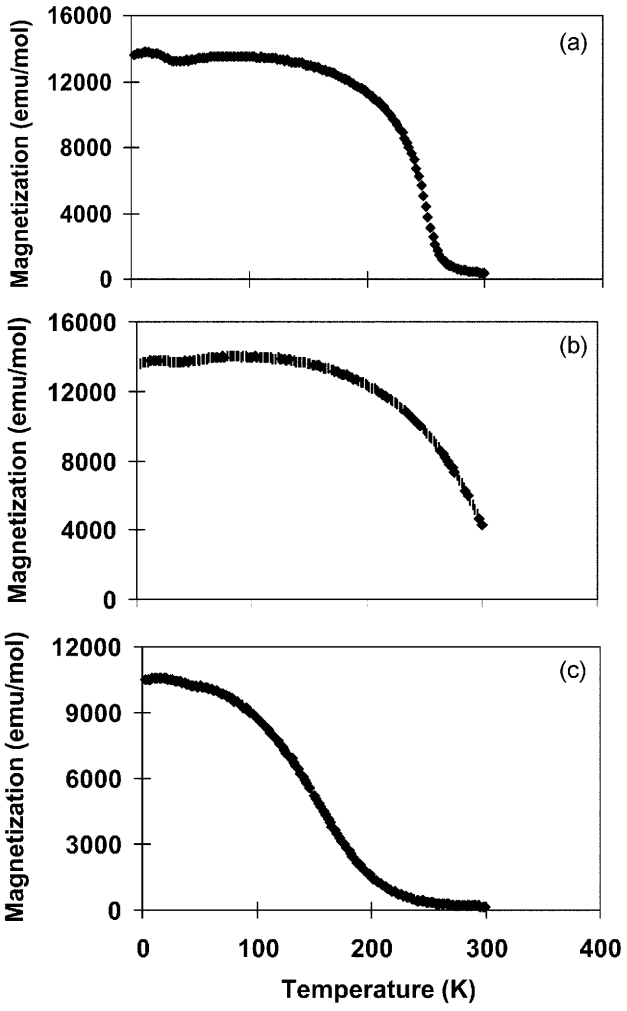

Figure 5. Temperature dependence of the magnetization of (**a**) $LaMnO_3$, (**b**) $La_{0.67}Sr_{0.33}MnO_3$ and (**c**) $La_{0.67}Ca_{0.33}MnO_3$ nanoparticles at 5 kOe.

4. Conclusions

Monophasic, homogeneous nanoparticles of $LaMnO_3$ (68 nm), $La_{0.67}Sr_{0.33}MnO_3$ (80 nm) and $La_{0.67}Ca_{0.33}MnO_3$ (50 nm) have been synthesised through a modified reverse micellar route for the first time using tergitol as the surfactant. Magnetization studies show the onset of ferromagnetic ordering at around 250 K for $LaMnO_3$, ~350 K for $La_{0.67}Sr_{0.33}MnO_3$ and 200 K for $La_{0.67}Ca_{0.33}MnO_3$ which indicate that the magnetic interactions found in the bulk appear to be retained at 50–80 nm grain size.

Acknowledgements

AKG thanks the Department of Science and Technology, Govt. of India for financial support. TA thanks Council of Scientific and Industrial Research, Govt. of India for a fellowship. SEL acknowledges support from the National Science Foundation, USA.

References

1. von Helmolt R, Wecker J, Holzapfel B, Schultz L and Samwer K 1993 *Phys. Rev. Lett.* **71** 2331
2. Levy P M 1992 *Science* **256** 972
3. Skinner S J 2001 *Fuel Cells Bull.* **4** 6
4. Ishihara T, Kilner J A, Honda M and Takia T 1997 *J. Am. Chem. Soc.* **119** 2747
5. Singhal S 2000 *MRS Bull.* **25** 16
6. Carvajal J R, Hennion M, Moussa F, Moudden A H, Pinsard L and Revcolevschi A 1998 *Phys. Rev.* **B57** R3189
7. Rao C N R, Cheetham A K and Mahesh R 1996 *Chem. Mater.* **8** 2421
8. Rao C N R and Cheetham A K 1997 *Adv. Mater.* **9** 1009
9. Komarneni S, D'Arrigo M C, Leionelli C, Pellacani G C and Katsuki H 1998 *J. Am. Ceram. Soc.* **81** 3041
10. Athawale A A and Bapat M 2005 *J. Metastable Nanocryst. Mater.* **23** 3
11. Chatterjee A, Das D, Pradhan S K and Chakravorty D 1993 *J. Magn. Magn. Mater.* **127** 214
12. Boutonnet M, Kizling J, Stenius P and Maire G 1982 *Coll. Surf.* **5** 209
13. Pileni M P 1993 *J. Phys. Chem.* **97** 6961
14. Steigerwald M L, Alivisatos A P, Gibson J M, Harris T D, Korbin R and Müller A J 1988 *J. Am. Chem. Soc.* **110** 3046
15. Zhang D, Qi L, Ma J and Cheng H 2002 *J. Mater. Chem.* **12** 3677

16. Chen D H and Wu S H 2000 *Chem. Mater.* **12** 1354
17. Ahmad T, Kavitha G, Narayana C and Ganguli A K 2005 *J. Mater. Res.* **20** 1415
18. Ahmad T and Ganguli A K 2006 *J. Am. Ceram. Soc.* **89** 1326
19. Ahmad T, Ramanujachary K V, Lofland S E and Ganguli A K 2004 *J. Mater. Chem.* **14** 3406
20. Lee Y C, Liang M H, Hu C T and Lin I N 2001 *Eur. Ceram. Soc.* **21** 2755
21. Giannakas A E, Ladavos A K and Pomonis P J 2004 *Appl. Catal.* **B49** 147
22. Uskokovic V, Makovec D and Drofenik M 2005 *Mater. Sci. Forum* **494** 155
23. Belevtsev B I, Naugle D G, Rathnayaka K D D, Parasiris A and Finowicki J F 2005 *Physica* **B355** 341
24. Dai P, Zhang J, Mook H A, Liou S H, Dowben P A and Plummer E W 1996 *Phys. Rev.* **B54** R3694
25. Urushibara A, Moritomo Y, Arima T, Asamitsu A, Kido G and Tokura Y 1995 *Phys. Rev.* **B51** 14103
26. Schiffer P, Ramirez A P, Bao W and Cheong S W 1995 *Phys. Rev. Lett.* **75** 3336
27. Van Santen J H and Jonker G H 1950 *Physica* **16** 599